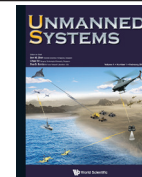


Unmanned Systems, Vol. 6, No. 3 (2018) 1–12
 © World Scientific Publishing Company
 DOI: 10.1142/S2301385018400095



UNMANNED SYSTEMS

<http://www.worldscientific.com/worldscinet/us>



Input and Output Constraints in Iterative Learning Control Design for Robotic Manipulators

Gijo Sebastian^{*,†}, Ying Tan^{*,§}, Denny Oetomo^{*,¶}, Iven Mareels^{†,||}

**School of Electrical, Mechanical and Infrastructure Engineering,
 The University of Melbourne, Parkville, Victoria 3010, Australia*

*†IBM Research — Australia, 60 City Road,
 Southbank Victoria 3006, Australia*

Motivated by the safety requirement of rehabilitation robotic systems for after stroke patients, this paper handles position or output constraints in robotic manipulators when the patients repeat the same task with the robot. In order to handle output constraints, if all state information is available, a state feedback controller can ensure that the output constraints are satisfied while iterative learning control (ILC) is used to learn the desired control input through iterations. By incorporating the feedback control using barrier Lyapunov function with feed-forward control (ILC) carefully, the convergence of the tracking error, the boundedness of the internal state, the boundedness of input signals can be guaranteed along with the satisfaction of the output constraints over iterations. The effectiveness of the proposed controller is demonstrated using simulations from the model of EMU, a rehabilitation robotic system.

Keywords: Iterative learning control; output constraints; barrier Lyapunov function.

US

1. Introduction

The idea of iterative learning control (ILC) was proposed in [1] for improving the tracking performance of robots which are operated in a repetitive fashion, i.e., the same task, the same system, and the same initial condition. Last three decades of extensive research in the domain of ILC has addressed multitude of challenges in the design, analysis and synthesis of this control technique. It also finds applications in batch manufacturing, chemical processing, modelling human motor learning, robotic rehabilitation and freeway traffic control (see survey papers [2–5] and references therein for more details on various theoretical developments and applications).

Motivated by the idea of “practice makes perfect”, an ILC algorithm usually uses the information of past and/or current performance, for example, the tracking error, and

past control efforts. For a task that is repetitive over a finite time interval $[0, T_f]$, a general form of updating law is given by

$$u_{i+1}(t) = u_i(t) + f_u(e_i(t), e_{i+1}(t)), \quad t \in [0, T_f],$$

where the subscript i denotes the signal at i th iteration and t denotes the time. The symbol u denotes the control input and e denotes the tracking error. As the repetitive features of the task have been explored, ILC can be considered as a “data-driven” method, which could relax the requirement of plant knowledge in the design of the controller [6].

In a standard analysis of stability or attractivity requirement of dynamic systems, the steady-state ($t \rightarrow \infty$) behaviors are important. The problem formulation of ILC would consider both finite time-domain and infinite iteration-domain. Mathematically, the convergence analysis is defined on a some functional space. Under such a situation, both strong convergence (uniform convergence) and weak convergence (point-wise convergence) can be used to characterize the convergence of an ILC algorithm [7]. Next, a brief literature review of different convergence analyses will be provided.

Received 26 April 2018; Revised 16 June 2018; Accepted 16 June 2018;
 Published xx xx xx. This paper was recommended for publication in its revised form by Guest Editors, Ying Tan and Qinyuan Tan.
 Email Addresses: [†]gsebastian@student.unimelb.edu.au, [§]yingt@unimelb.edu.au, [¶]doetomo@unimelb.edu.au, ^{||}imareels@au1.ibm.com

1.1. Literature review

Based on two different convergence conditions, there are two major analysis tools to check the convergence of closed loop continuous-time dynamic systems: contraction mapping (CM)-based method and “energy”-like function (EF) based techniques [8].

CM-based methods were motivated from the pioneering works in [1] and are able to achieve uniform convergence of the tracking error. In order to obtain this stronger convergence property, the system of interest has to satisfy strong assumptions. For example, the function in the system dynamic equation might need to satisfy global Lipschitz continuity (GLC) condition.

The “energy”-like functions (EFs) have been used in [9–11]. Usually, EF is defined in \mathcal{L}^2 , leading to point-wise convergence.

The concept of composite energy function (CEF) is later introduced by one of pioneers in ILC domain, Professor Xu and his coauthor in [12], which incorporates a Lyapunov function and \mathcal{L}^2 norm (or \mathcal{L}^2 norm equivalent) of learning parameters [13–15]. Commonly in CEFs, Lyapunov function is related to the performance in the finite time-domain while the \mathcal{L}^2 norm of learning parameters captures the learning in the iteration-domain [7]. With the weak convergence condition, the CEF-based design can be easily applied to dynamic systems without satisfying GLC. For example, this technique has been employed to learn parametric uncertainties [12], to handle nonparametric uncertainties [15], and to handle input saturation [14] as well.

It is worthwhile to highlight that two different approaches (CM-based ILC and EF or CEF-based ILC) can be unified under CEF-based approach. In [16], a CEF is used to show the convergence of an ILC algorithm that is designed by CM-based method.

1.2. Motivation and control objective

The motivation of this work comes from the design of a rehabilitation robotic system that can provide intelligent assistance for after stroke patients to recover through repetitive rehabilitation exercises. Post-stroke patients often suffer from movement impairments of their limbs. Therapy generally involves repetitive exercises of the affected limb for basic movements with associated functional goals [17]. With the consideration of the safety of patients, there is a safe region unique to each patient based on his or her ability to move [18]. Violating this safety region of operation may overstretch the patient causing injuries, or collision with face or torso. For a specific patient, for a given trajectory, the safety region becomes time-varying. Moreover, the assistance coming from robotic systems is generated by motors with the bounded torque. This motivates the

following control objective: For a given repetitive task, design an appropriate bounded control input, which can drive the output to the desired trajectory without violating the time-varying output constraints.

Most engineered systems are subjected to the input constraints and/or the state/output constraints due to physical limitations of the systems. In ILC, input constraints have been exploited in [14, 16, 19]. On the other hand, in chemical processes or robotic manipulators, the safety requirements normally require the output constraints to be satisfied [20, 21]. Compared with input constraints, there has been not much work in dealing with output constraints in the domain of ILC.

It is worthwhile to highlight that barrier Lyapunov function has been widely used to design other learning control settings in order to satisfy the state/output constraints in [22–24]. In those works, the barrier Lyapunov function technique has been implemented to handle state/output constraints for repetitive learning systems, in which the trajectories are periodic in t . Under such a situation, the stability analysis tools used [25] can be used as only time-domain performance is required.

In our previous work [26], the time-invariant output constraints were handled by using a full state-feedback designed using barrier-function based CEF. It has been shown that the output constraints can be satisfied with the bounded energy of feed-forward control input, leading to the possibility of having unbounded input signals.

This work extends our previous work [26] to address time-varying output constraints. A soft constraint of ILC has been added to ensure that the control input is uniformly bounded over the iteration-domain. Hence, both hard output constraints and soft input constraints are addressed in this paper.

1.3. Contributions

The contribution of this paper is two-fold:

- (i) A new fictitious velocity is introduced in feedback-based ILC scheme to satisfy the time varying output constraints in robotic manipulators.
- (ii) A soft constraint has been added in the ILC design to ensure that the control input is uniformly bounded over iterations.

The paper is organized as follows. The preliminaries are introduced in Sec. 2. Section 3 provides the plant model, required assumptions, and the control objective. The proposed control scheme and the main result are given in Sec. 4. The proof of the main result is given in Appendix B. The effectiveness of proposed control architecture is demonstrated in Sec. 5 using a simulation on a three degrees of freedom model of robot.

2. Preliminaries

The following notations are used in this paper. \mathcal{R} denotes the set of real numbers. \mathcal{N} denotes the set of natural numbers. The set of all continuous functions in $[0, T_f]$ that are differentiable up to j th order is denoted by $\mathcal{C}^j[0, T_f]$ for any $j \in \mathcal{N}$.

For a vector $\mathbf{x} \in \mathcal{R}^n$, $|\mathbf{x}|$ denotes the Euclidean norm as $|\mathbf{x}|^2 = \mathbf{x}^\top \mathbf{x}$. For a given matrix $A \in \mathcal{R}^{n \times m}$, $|A|$ indicates the induced matrix norm. A square matrix $A = A^\top > (\geq) 0$ indicates that this matrix is symmetric and positive definite (positive semi-definite). For a square matrix, the notion of $\lambda_{\min}(A)$ stands for the minimum eigenvalue of A . If matrix $A \in \mathcal{R}^{n \times n}$ is skew-symmetric, then $A^\top = -A$. The identity matrix of dimension n is denoted by I_n .

The following definitions will be used later.

Definition 1. A function $\mathbf{f}(\cdot, \cdot)$ is said to be *locally Lipschitz continuous* on a domain (open and connected set) $\mathcal{D} \subset \mathcal{R}^n$ if for each point in \mathcal{D} , it has a neighborhood \mathcal{D}_0 such that there exists $L_0 = L_0(\mathcal{D}_0)$ such that the following inequality holds:

$$|\mathbf{f}(\mathbf{x}_1, \mathbf{y}_1) - \mathbf{f}(\mathbf{x}_2, \mathbf{y}_2)| \leq L_0(|\mathbf{x}_1 - \mathbf{x}_2| + |\mathbf{y}_1 - \mathbf{y}_2|), \quad (1)$$

for all points $\mathbf{x}_1, \mathbf{x}_2, \mathbf{y}_1, \mathbf{y}_2 \in \mathcal{D}_0$.

Definition 2. Let u^* be a positive constant. The saturation function is defined as $\text{sat}(u, u^*) \triangleq \text{sign}(u) \min\{u^*, |u|\}$ for any $u \in \mathcal{R}$.

Let $\mathbf{u}^* \in \mathcal{R}^m$ be a positive vector with every element positive. For any $\mathbf{u} \in \mathcal{R}^m$, $\text{sat}(\mathbf{u}, \mathbf{u}^*) = [\text{sat}(u^1, u^{1*}), \dots, \text{sat}(u^m, u^{m*})]^\top$.

Definition 3. For any $\mathbf{x}(\cdot) \in \mathcal{C}[0, T_f]$, the supremum norm is defined as $\|\mathbf{x}_s\| \triangleq \max_{t \in [0, T_f]} |\mathbf{x}(t)|_\infty$, where $|\mathbf{x}|_\infty = \max_{j \in [1, n]} |x^j|$ and x^j denotes j th element of \mathbf{x} .

Definition 4. For any $\mathbf{x}(\cdot) \in \mathcal{C}[0, T_f]$ the \mathcal{L}^2 norm is defined as $\|\mathbf{x}\|_{\mathcal{L}^2} \triangleq (\int_0^{T_f} |\mathbf{x}(\tau)|^2 d\tau)^{\frac{1}{2}}$ where as the \mathcal{L}_e^2 norm is defined as $\|\mathbf{x}\|_{\mathcal{L}_e^2} \triangleq (\int_0^{T_f} e^{-\lambda\tau} |\mathbf{x}(\tau)|^2 d\tau)^{\frac{1}{2}}$, for any $\lambda > 0$.

Lemma 1 will be used to facilitate the proof of the main result.

Lemma 1 ([14, Property-3]). For any given \mathbf{u}_r, \mathbf{u} and $\mathbf{u}^* \in \mathcal{R}^m$ satisfying $\text{sat}(\mathbf{u}_r, \mathbf{u}^*) = \mathbf{u}_r$ then the following inequality holds true: $|\mathbf{u}_r - \text{sat}(\mathbf{u}, \mathbf{u}^*)|^2 \leq |\mathbf{u}_r - \mathbf{u}|^2$.

3. Problem Formulation

A lumped parametric model of robotic systems is introduced in this Section, followed by the assumptions required and the control objective.

3.1. Plant model

The equations of motion of a revolute, direct-drive robotic manipulator with n rigid links is given by [27]

$$M(\boldsymbol{\theta})\ddot{\boldsymbol{\theta}} + C(\boldsymbol{\theta}, \dot{\boldsymbol{\theta}})\dot{\boldsymbol{\theta}} + \mathbf{f}(\dot{\boldsymbol{\theta}}) + \mathbf{g}(\boldsymbol{\theta}) = \mathbf{u}, \quad (2)$$

where $\boldsymbol{\theta}, \dot{\boldsymbol{\theta}}$ and $\ddot{\boldsymbol{\theta}} \in \mathcal{R}^n$ are the vector of joint angles, velocities and accelerations respectively. $\mathbf{u} \in \mathcal{R}^n$ is the vector of joint torque. $M(\cdot) \in \mathcal{R}^{n \times n}$ is the inertial matrix, $C(\cdot, \cdot) \in \mathcal{R}^{n \times n}$ represents the total Coriolis and centripetal terms, $\mathbf{f}(\cdot) \in \mathcal{R}^n$ is the friction component and $\mathbf{g}(\cdot) \in \mathcal{R}^n$ is the gravity force vector.

Remark 1. The problem formulation is based on robotic manipulators. This is motivated from the rehabilitation robotic systems as indicated in Introduction. However, the proposed control design methods can be equally applicable to more general nonlinear systems.

It is assumed that the exact model parameters are unknown to the designer; however, the system (2) exhibits the following properties [27]. These properties will be used in the proof of the main result.

Property 1. For any $\boldsymbol{\theta} \in \mathcal{R}^n$, the inertial matrix $M(\boldsymbol{\theta}) = M^\top(\boldsymbol{\theta}) > 0$. Moreover, there exist positive constants $\mu_1 > 0$ and $\mu_2 > 0$, such that $0 < \mu_1 I_n \leq M(\boldsymbol{\theta}) \leq \mu_2 I_n$.

Property 2. For any $\boldsymbol{\theta} \in \mathcal{R}^n$, $(\dot{M}(\boldsymbol{\theta}) - 2C(\boldsymbol{\theta}, \dot{\boldsymbol{\theta}}))$ is a skew symmetric matrix. Therefore, $\boldsymbol{\theta}^\top (\dot{M} - 2C)\boldsymbol{\theta} = 0$.

Property 3. There exist three positive constants: C_b , F_b , and G_b such that: $|C(\boldsymbol{\theta}, \dot{\boldsymbol{\theta}})| \leq C_b |\dot{\boldsymbol{\theta}}|$, $|\mathbf{f}(\dot{\boldsymbol{\theta}})| \leq F_b |\dot{\boldsymbol{\theta}}|$ and $|G(\boldsymbol{\theta})| \leq G_b$.

The system dynamics (2) can be represented by a multiple-input-multiple-output (MIMO) square^a system:

$$\begin{pmatrix} \dot{\mathbf{x}}_{1,i} \\ \dot{\mathbf{x}}_{2,i} \end{pmatrix} = \begin{pmatrix} \mathbf{x}_{2,i} \\ \mathbf{h}(\mathbf{x}_{1,i}, \mathbf{x}_{2,i}) \end{pmatrix} + \begin{pmatrix} 0 \\ M^{-1}(\mathbf{x}_{1,i}) \end{pmatrix} \mathbf{u}_i \quad (3)$$

$$\mathbf{y}_i = \mathbf{x}_{1,i},$$

where

$$\begin{aligned} \mathbf{h}(\mathbf{x}_{1,i}, \mathbf{x}_{2,i}) \triangleq & -M^{-1}(\mathbf{x}_{1,i})C(\mathbf{x}_{1,i}, \mathbf{x}_{2,i})\mathbf{x}_{2,i} \\ & - M^{-1}(\mathbf{f}(\mathbf{x}_{2,i}) + \mathbf{g}(\mathbf{x}_{1,i})). \end{aligned}$$

Here, $(\cdot)_i$ represents the variable at the i th iteration, $\mathbf{x}_{1,i} = \boldsymbol{\theta}_i$ and $\mathbf{x}_{2,i} = \dot{\boldsymbol{\theta}}_i$. It is noted that the system (3) has a relative degree two. As pointed out in [7, 28], this information is needed in the design of ILC.

Assumption 1. There exists reference output $\mathbf{y}_r = \mathbf{x}_{1,r} \in \mathcal{C}^2[0, T_f]$, with reference state $\mathbf{x}_{2,r} \in \mathcal{C}^1[0, T_f]$ and

^aA square system has same the dimension for input and output vectors.

reference input $\mathbf{u}_r \in \mathcal{C}[0, T_f]$ that satisfy

$$\begin{pmatrix} \dot{\mathbf{x}}_{1,r} \\ \dot{\mathbf{x}}_{2,r} \end{pmatrix} = \begin{pmatrix} \mathbf{x}_{2,r} \\ \mathbf{h}(\mathbf{x}_{1,r}, \mathbf{x}_{2,r}) \end{pmatrix} + \begin{pmatrix} \mathbf{0} \\ M^{-1}(\mathbf{x}_{1,r}) \end{pmatrix} \mathbf{u}_r, \quad (4)$$

$$\mathbf{y}_r = \mathbf{x}_{1,r}.$$

Moreover, there exists a known positive vector \mathbf{u}^* such that $\text{sat}(\mathbf{u}_r, \mathbf{u}^*) = \mathbf{u}_r, \forall t \in [0, T_f]$ is satisfied.

Remark 2. It is noted that an ILC algorithm usually serves as an integrator in the iteration-domain (see the general form of ILC in Introduction). Hence, the control input might become unbounded as the number of iterations goes to infinity. In order to avoid unbounded control input, a soft input constraint is introduced. Our future work will consider hard constraints on input (actuator constraint) and output signals.

The tracking error is defined as $\mathbf{e}_i(t) \triangleq \mathbf{y}_r(t) - \mathbf{y}_i(t), \forall t \in [0, T_f]$ for any iteration i .

Assumption 2. The system (3) executes repetitive tracking over a fixed time interval $[0, T_f]$, satisfying the identical initial condition at every iteration, where $\mathbf{e}_i(0) = \dot{\mathbf{e}}_i(0) = \ddot{\mathbf{e}}_i(0) = \mathbf{0}, \forall i \in \mathcal{N}$.

Remark 3. Assumption 2 is a standard assumption in the ILC as indicated in [7]. It is possible to relax this assumption by compensating the perfect tracking performance. Apart from identical initial condition, five different resetting conditions are discussed with different performance observed in [29]. Moreover for robotic manipulators, it is often feasible to reset position, velocity and acceleration.

3.2. Control objective

The control objective is to find a sequence of control input $\{\mathbf{u}_i\}_{i \in \mathcal{N}}$ such that the tracking error \mathbf{e}_i converges to zero uniformly and the output at each iteration i satisfies the constraint, i.e., $(\mathbf{y}_i(t))^\top \mathbf{y}_i(t) \leq k_b^2(t), \forall t \in [0, T_f], \forall i \in \mathcal{N}$.

For a given task space, the safety region is defined *a priori*. For each given task, in order to ensure that the output trajectories will stay in the safety region, a time-varying output constraint is obtained. That is for a given $\mathbf{y}_r \in \mathcal{C}^2[0, T_f]$, there exists a $k_b(\cdot) \in \mathcal{C}[0, T_f]$ such that $|\mathbf{y}(t)| \leq k_b(t)$, where $k_b(t) > 0$ defines the bound for output trajectories. For any given $k_b(t)$ and desired reference trajectory $\mathbf{y}_r(t)$, there exists a time-varying error bound $\varepsilon_b(t) > 0$ such that if $\mathbf{e}_i^\top(t) \mathbf{e}_i(t) \leq \varepsilon_b^2(t)$ is satisfied, the output constraints at the joint level will not be transgressed.

Hence, the control objective can be redefined as achieving the perfect tracking performance without violating the time-varying output error bound. More precisely, the control objective is to design a sequence of control input

$\{\mathbf{u}_i\}_{i \in \mathcal{N}}$ such that $\mathbf{e}_i^\top(t) \mathbf{e}_i(t) \leq \varepsilon_b^2(t), \forall i \in \mathcal{N}$ and $\lim_{i \rightarrow \infty} |\mathbf{e}(t)| = \mathbf{0}$ point-wisely.

Remark 4. It is noted that a time-invariant output constraint at joint space will also result in a time-varying output error bound for a given time-varying reference trajectory. For example, when a constant k_b is selected, i.e., $k_b > |\mathbf{y}_r(t)|_\infty$ for all $t \in [0, T_f]$, it leads to a time-varying error bound $\varepsilon_b(t)$, i.e., $\varepsilon_b(t) = k_b - |\mathbf{y}_r(t)|_\infty$.

4. Controller Design

The proposed control architecture is shown in Fig. 1. It consists of a feedback control coupled with a feed-forward ILC. The role of feedback controller is to cope with time-varying output constraints while the feed-forward ILC “learns” the desired input signal. The feedback controller is designed using a barrier function like Lyapunov function (BF-LF), similar to [24, 23]. As far as the finite time-domain is considered, the proposed BF-LF will lead to the satisfaction of hard output constraints. But it is not sufficient to ensure the perfect tracking performance. Once the output constraints are satisfied within the bounded state, the feed-forward ILC ensures the convergence of tracking error.

It is noted that though a special form of BF-LF is used, the analysis tool presented can be applied when other design techniques or other BF-LFs are used.

The overall control input can be calculated as:

$$\mathbf{u}_i(t) = \tilde{\mathbf{u}}_i^{ff}(t) + \mathbf{u}_i^{fb}(t), \quad \forall t \in [0, T_f], i \in \mathcal{N}, \quad (5)$$

where $\tilde{\mathbf{u}}_i^{ff}(t) = \text{sat}(\mathbf{u}_i^{ff}(t), \mathbf{u}^*)$ represents a modified feed-forward control input and $\mathbf{u}_i^{fb}(t)$ represents a stabilizing feedback control based on BF-LF.

Next subsections will provide more details on ILC design and feedback design.

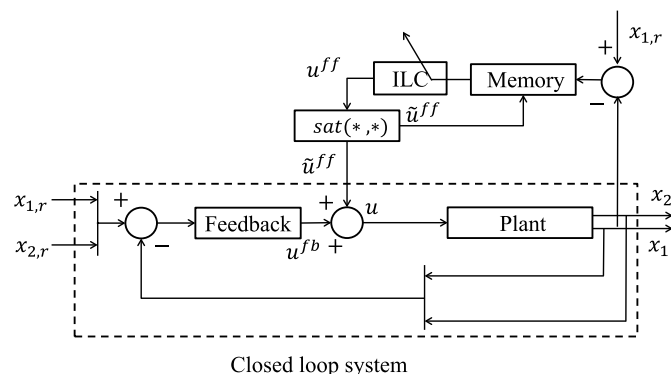


Fig. 1. Block diagram of proposed control architecture.

4.1. Design of ILC

The proposed ILC is given by

$$\mathbf{u}_{i+1}^{ff}(t) = \tilde{\mathbf{u}}_i^{ff}(t) + q\Gamma(t)\dot{\mathbf{e}}_i(t), \quad \mathbf{u}_1^{ff}(t) = 0, \quad (6)$$

where $\Gamma(t) \in \mathcal{R}^{n \times n}$ is a positive definite matrix and $q > 0$ is the learning rate.

Remark 5. The proposed ILC (6) is a modified form of standard ILC proposed in [28] for a MIMO square system with a relative degree of two. With an appropriate convergence condition (see Theorem 1), it is possible to show that the proposed feed-forward ILC can ensure the perfect tracking performance as iteration goes to infinity as well as the boundedness of input signals over iterations. The role of introducing the saturation function is to force the feed-forward control input to remain in a bounded set for any iteration. Similar updating law has been previously proposed in [30]. In most of the practical implementations, these bounds on control input are known *a priori* as it is directly related to the physical limits of actuators.

4.2. Design of feedback control

A new fictitious tracking error is introduced in this section to facilitate the design and analysis of feedback controller. The fictitious velocity error $\boldsymbol{\sigma}$ is given by

$$\boldsymbol{\sigma} \triangleq \dot{\mathbf{e}} + \cos^2\left(\frac{\pi \mathbf{e}^\top \mathbf{e}}{2\varepsilon_b^2}\right) K_1 \mathbf{e} - \frac{\dot{\varepsilon}_b}{\varepsilon_b} \mathbf{e} + \frac{\dot{\varepsilon}_b \varepsilon_b}{\pi \mathbf{e}^\top \mathbf{e}} \sin\left(\frac{\pi \mathbf{e}^\top \mathbf{e}}{\varepsilon_b^2}\right) \mathbf{e},$$

for all $t > 0$, $\boldsymbol{\sigma}(0) = 0$,

(7)

where the matrix $K_1 \in \mathcal{R}^{n \times n}$ is symmetric positive definite. Note that $\varepsilon_b(\cdot) \neq 0$, the new velocity error $\boldsymbol{\sigma}$ is well-defined.

Remark 6. It can be shown that

$$\lim_{\mathbf{e} \rightarrow 0} \left[-\frac{\dot{\varepsilon}_b}{\varepsilon_b} \mathbf{e} + \frac{\dot{\varepsilon}_b \varepsilon_b}{\pi \mathbf{e}^\top \mathbf{e}} \sin\left(\frac{\pi \mathbf{e}^\top \mathbf{e}}{2\varepsilon_b^2}\right) \mathbf{e} \right] = 0, \quad (8)$$

which indicates that the singularity will not happen when \mathbf{e} approaches zero. However, when computing this signal numerically, it is possible that some numerical error will lead to a very large value of $\boldsymbol{\sigma}$. In order to avoid this from happening, it is possible to set $\boldsymbol{\sigma}$ as zero when the tracking error is sufficiently small. For example, $\boldsymbol{\sigma} = \mathbf{0}$ if $|\mathbf{e}| < \varepsilon_0$ where ε_0 is a sufficiently small positive number.

The proposed feedback control \mathbf{u}^{fb} has the following form:

$$\mathbf{u}^{fb} = K_2 \boldsymbol{\sigma} + \sec^2\left(\frac{\pi \mathbf{e}^\top \mathbf{e}}{2\varepsilon_b^2}\right) \mathbf{e}, \quad (9)$$

where $K_2 \in \mathcal{R}^{n \times n}$ is also a symmetric positive definite matrix satisfying $\lambda_{\min}(K_2) > 1$.

Remark 7. If no output constraint is considered in the analysis, then $k_b(t) \rightarrow \infty$ leads to $\varepsilon_b(t) \rightarrow \infty$ for all t . It is not difficult to show $\lim_{\varepsilon_b \rightarrow \infty} \mathbf{u}^{fb} = K_2 K_1 \mathbf{e} + \mathbf{e} + K_2 \dot{\mathbf{e}}$. This indicates that one major role of the feedback law (9) is to stabilize the system as it is equivalent to a PD-type control when there is no output constraint.

Remark 8. In the proof of the main result, it will show that the main role of the feedback law (9) is to ensure that the output constraints are satisfied. It is designed based on the concept of barrier function, which will approach to infinity when the output approaches the constraints. The barrier function will drive the trajectories of the dynamic systems away when they are going to hit the constraints [31].

Remark 9. The design of feedback is based on the choice of a barrier function. This work adopts a tan-type barrier function proposed by Professor Xu in [22], and the BF-LF is given by

$$V(\mathbf{e}, \boldsymbol{\sigma}) \triangleq \frac{\varepsilon_b^2}{\pi} \tan\left(\frac{\pi \mathbf{e}^\top \mathbf{e}}{2\varepsilon_b^2}\right) + \frac{1}{2} \boldsymbol{\sigma}^\top M(\mathbf{x}_1) \boldsymbol{\sigma},$$

$$|\mathbf{e}(0)| \leq \max_{t \in [0, T_f]} |\varepsilon_b(t)|. \quad (10)$$

Other barrier functions (for example, a log barrier function proposed in [32]) can be used in the design of a feedback controller. The similar analysis procedure can be directly applied to show the convergence and the satisfaction of the output constraints.

Remark 10. Using L'Hospital's rule, it can be shown that: $\lim_{\varepsilon_b \rightarrow \infty} \frac{\varepsilon_b^2}{\pi} \tan\left(\frac{\pi \mathbf{e}^\top \mathbf{e}}{2\varepsilon_b^2}\right) = \frac{1}{2} \mathbf{e}^\top \mathbf{e}$. Therefore, BF-LF is equivalent to a quadratic function in \mathbf{e} and $\dot{\mathbf{e}}$, when the constraints are neglected.

When only the feedback (9) is used, Proposition 1 shows that the output constraints are satisfied.

Proposition 1. For the system (3) satisfying Assumption 2 with the feedback control law (9), the constraints $|e(t)| \leq \varepsilon_b(t)$ are always satisfied for any $t \geq 0$ when $\mathbf{u}^{ff} = \mathbf{0}$

Proof. The proof of Proposition 1 is presented in Appendix A. \square

Due to existence of feed-forward ILC, it is possible that in some iterations, the output constraints might be violated. On the other hand, the existence of feedback control law might cause trouble in the convergence analysis in the iteration-domain. How to ensure the convergence of the tracking error as well as the satisfaction of the output constraints? Next subsection will present the main result of this paper to show convergence.

4.3. Convergence of proposed learning control

The main result of this paper present the convergence condition to show that the proposed controller (5) can achieve the perfect tracking performance as $i \rightarrow \infty$. Moreover, the hard output constraints are satisfied and the control input is bounded for all iterations.

Theorem 1. *The system (3) with the control laws (5), (9) and (6) under the Assumptions 1 and 2:*

- (i) *Satisfies the output constraints $|\mathbf{e}_i(t)| \leq \varepsilon_b(t)$ for all $t \in [0, T_f]$ and $i \in \mathcal{N}$;*
- (ii) *Can achieve zero output tracking error, i.e., $\lim_{i \rightarrow \infty} \mathbf{e}_i(t) \rightarrow \mathbf{0}$ uniformly;*
- (iii) *The feed-forward control input \mathbf{u}_i^{ff} converges to the reference input \mathbf{u}_r in \mathcal{L}^2 norm sense;*
- (iv) *and the control input \mathbf{u}_i defined in (5) is uniformly bounded for any i ,*

if the convergence condition:

$$|I_n - q\Gamma(t)M^{-1}(\mathbf{x}_1(t))| < 1, \forall t \in [0, T_f] \quad (11)$$

is satisfied.

Proof. The proof of Theorem 1 is presented in Appendix B. \square

A composite energy function, motivated from the works of Professor Xu [12], will be used to show the convergence of tracking error.

The proof of Theorem 1 uses induction. Clearly at the first iteration, there is no feed-forward ILC. Under such a situation, the feedback control law will ensure that the output constraints are satisfied.

At the second iteration, it will show that the proposed control law (5) will be lead to nonincreasing CEF along iteration-domain.

It is noted that the novelty of this induction is to show that the needed state will be in a compact set, which is iteration invariant. Finding such a compact set plays an important role in the analysis.

By using induction technique, it can be shown that the proposed control law (5) ensures the convergence of tracking error in iteration-domain without violating the output constraints.

5. An Illustrative Example

The model of a three degree of freedom rehabilitation robot EMU, (The University of Melbourne, Australia [33]) is used for the simulation. The schematics of the robot is shown in Fig. 2.

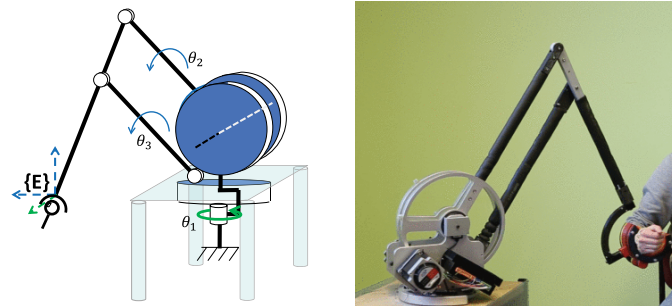


Fig. 2. EMU — a rehabilitation robot with $\theta_1, \theta_2, \theta_3$ are the actuated degrees of freedom with a passive spherical wrist.

The patient's forearm is attached to the robot end effector, $\{\mathbf{E}\}$ with a passive spherical joint, simulating a point of contact between the robot and the human arm. For the purpose of simulation and to illustrate the main idea presented in this paper, the robotic manipulator model of EMU with the actuated degrees of freedom is considered in this section.

Assume the vector of joint angles are given by $\boldsymbol{\theta} = [\theta_1, \theta_2, \theta_3]^T$. The inertial matrix, the Coriolis and Centripetal force vector and the gravitational force vector are given by

$$M(\boldsymbol{\theta}) = \begin{bmatrix} m_1 & 0 & 0 \\ 0 & P_5 & P_4 \sin(\theta_2 - \theta_3) \\ 0 & P_4 \sin(\theta_2 - \theta_3) & P_6 \end{bmatrix}, \quad (12)$$

$$C(\boldsymbol{\theta}, \dot{\boldsymbol{\theta}})\dot{\boldsymbol{\theta}} = \begin{bmatrix} 2\dot{\theta}_1\dot{\theta}_2 \cos(\theta_2)(P_4 \cos(\theta_3) - P_3 \sin(\theta_2)) \\ -2\dot{\theta}_1\dot{\theta}_3 \sin(\theta_3)(P_2 \cos(\theta_3) + P_4 \sin(\theta_2)) \\ \frac{P_3}{2}\dot{\theta}_1^2 \sin(2\theta_2) - P_4\dot{\theta}_3^2 \cos(\theta_2 - \theta_3) \\ -P_4\dot{\theta}_1^2 \cos(\theta_2) \cos(\theta_3) \\ P_4\dot{\theta}_2^2 \cos(\theta_2 - \theta_3) \\ +\dot{\theta}_1^2 \sin(\theta_3)(P_2 \cos(\theta_3) + P_4 \sin(\theta_2)) \end{bmatrix}, \quad (13)$$

$$\mathbf{g}(\boldsymbol{\theta}) = \begin{bmatrix} 0 \\ P_7 \sin(\theta_2) \\ P_8 \cos(\theta_3) \end{bmatrix}, \quad (14)$$

where $m_1 = P_1 + P_2 \cos^2(\theta_3) + P_3 \cos^2(\theta_2) + 2P_4 \cos(\theta_3) \sin(\theta_2)$.

The frictional force vector is given by $\mathbf{f} = F_c \dot{\boldsymbol{\theta}}$, where F_c is a diagonal matrix with elements $[P_9, P_{10}, P_{11}]$.

The system identification has been performed to estimate the nominal parameters of the model. For more details on lumped mass modeling and system identification,

refer [34] and references therein. The model parameters are identified from experiments as $P_1 = 0.66$, $P_2 = 0.42$, $P_3 = -0.63$, $P_4 = 0.34$, $P_5 = 0.44$, $P_6 = 0.38$, $P_7 = -6.36$, $P_8 = -3.66$, $P_9 = 4.67$, $P_{10} = 1.63$, $P_{11} = 3.75$.

The magnitude of joint angles are desired to be less than 1.5 radians, therefore $k_b = 1.5$ is taken as the output constraint.

For the simulation, the desired trajectories are taken as $\mathbf{y}_r(t) = [y_{r_1}(t), y_{r_2}(t), y_{r_3}(t)]^\top$, where $y_{r_1}(t) = 0.5\sin^3(\pi\frac{t}{3})\cos(\pi\frac{t}{3})$, $y_{r_2}(t) = 0.4\sin^3(\pi\frac{t}{3}) + 0.7$, $y_{r_3}(t) = 0.4\sin^3(\pi\frac{t}{3}) + 0.6$. It is verified that the reference trajectory satisfies Assumption 1. For the given reference trajectory, the error bound is taken as per Remark 4. The simulation is performed with sampling time of 1 millisecond, i.e., $\Delta t = 0.001$ s.

In order to demonstrate the theoretical findings of this paper, the following simulations are performed. Firstly, ILC is designed and its performance in the iteration domain is investigated without considering the output constraints. Secondly, the performance of feedback controller is discussed to verify Proposition 1. Thirdly, the effectiveness of proposed control structure is discussed in detail.

5.1. Convergence of ILC without feedback

Tracking with ILC is performed without the feedback control where a finite time interval, T_f is selected as 3.

The soft constraint on input is taken as $\mathbf{u}^* = [12, 12, 12]$. The convergence condition (11) is satisfied if the updated rate, $q = 0.5$ and learning gain $\Gamma =$

$$\begin{bmatrix} 0.504 & 0 & 0 \\ 0 & 0.394 & -0.124 \\ 0 & -0.124 & 0.342 \end{bmatrix}$$

are used for the ILC law. For calculating the derivative from the output error \mathbf{e} , the backward difference method is used followed by passing through a butter-worth filter of order-4 and cut-off frequency 275 Hz. A high cut-off frequency has been selected for filter design to avoid distortion of signals in numerical calculation. The simulation is performed for 250 iterations without a feedback control. The supremum norm of the error $\|\mathbf{e}_i\|_s$ is plotted in Fig. 3 to show the convergence. It is observed that the output constraints are not satisfied for the first 40 iterations, even though convergence of tracking error can be achieved by an ILC law.

5.2. Time-domain performance of feedback control

The simulation is performed using the proposed feedback controller without any ILC controller. The intention is to show that the constraints are satisfied and there exists a lower bound $\bar{\nu} > 0$ such that $\lim_{t \rightarrow \infty} |\mathbf{e}|_\infty \geq \bar{\nu}$ (for more details on boundedness of ψ , refer Appendix A).

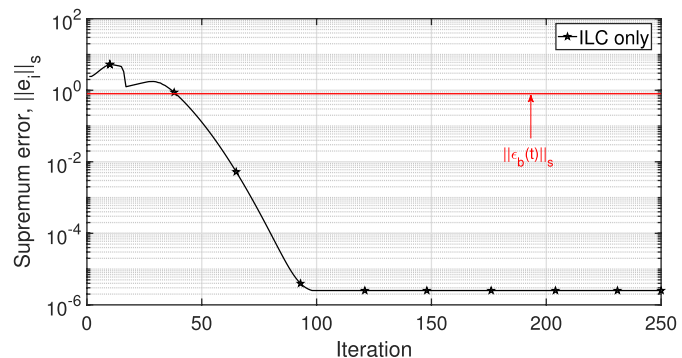


Fig. 3. Supremum norm of the output tracking error, $\|\mathbf{e}_i\|_s$ without feedback.

The feedback gains K_1 and K_2 are chosen as diagonal matrices with element $[9, 6, 6]$ and $[3, 3, 4.8]$, respectively. The simulation is performed for $T_f = 20$. The output trajectories are plotted in Fig. 4. It can be observed that the trajectories satisfy the time varying error bound $\varepsilon_b(t)$. However, the perfect tracking performance cannot be obtained. The variation of feedback control input is shown in Fig. 5. Clearly, the feedback control input is bounded in the time domain.

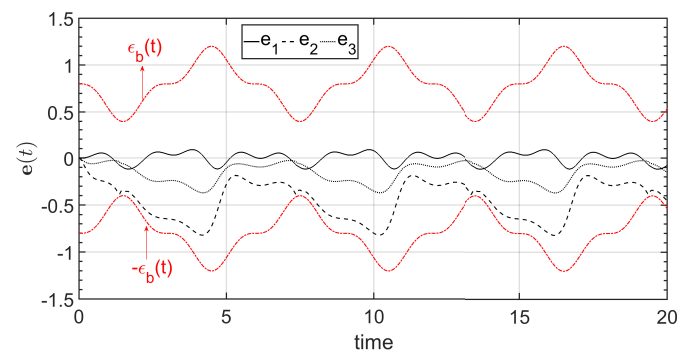


Fig. 4. Variation of tracking error in time for the proposed feedback.

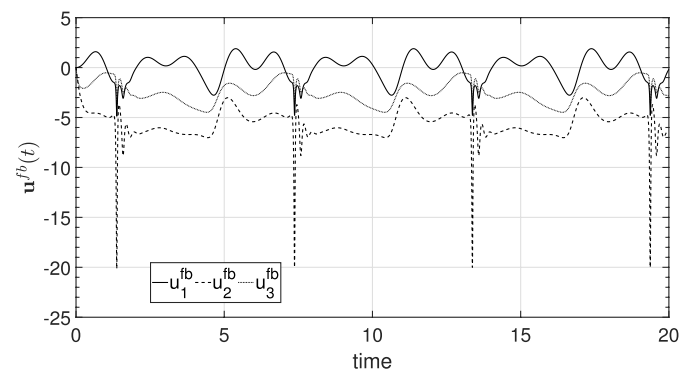


Fig. 5. Variation of control input in time for the proposed feedback.

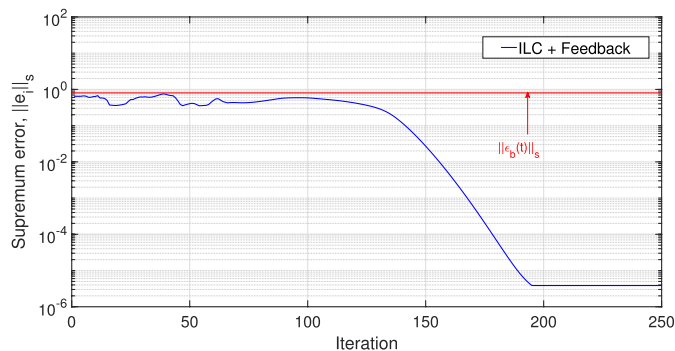


Fig. 6. Supremum norm of the output tracking error, $\|\mathbf{e}_i\|_s$ for the proposed controller.

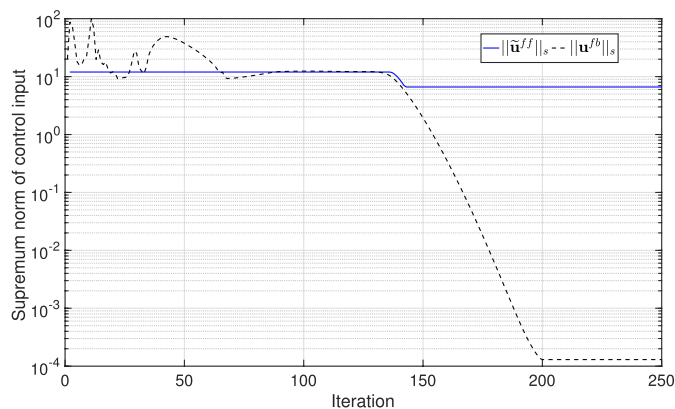


Fig. 7. Supremum norm of the error in control input, $\|\mathbf{u}_i^{fb}\|_s$ and $\|\tilde{\mathbf{u}}_i^{ff}\|_s$ for the proposed controller.

5.3. Convergence in the proposed control structure

The proposed controller (5) with the feedback controller (9) and feed-forward ILC (6) is applied to the simulation model with the controller parameters given in Secs. 5.1 and 5.2.

It is observed that the tracking error converges in iteration-domain and the output constraints are satisfied for any iteration as shown in Fig. 6. Figure 7 also shows that the feedback control approaches zero and feed-forward control input is bounded within the soft input constraints. This simulation shows the effectiveness of the proposed control algorithm.

6. Conclusion

A new feedback-based ILC scheme is proposed in this paper to handle the output constraints and soft input constraints for robotic manipulators and track the desired trajectory. The feedback in time-domain is designed with the help of a

barrier function like Lyapunov function, which can ensure the satisfaction of the output constraints in time-domain. By incorporating this barrier function like Lyapunov function into the composite energy function, it is shown that the proposed control law is able to track the desired trajectory perfectly and satisfy the output constraints with the bounded control input. The future work aims at extending the proposed ILC architecture to include both position constraints and the hard input constraints (from the actuator limits) with experimental validation on EMU.

Acknowledgments

This research is supported by the Australian Research Council under the Discovery Grant DP160104018.

The author, Ying Tan, would like to dedicate this work to her PhD supervisor and a long-time collaborator, the late Professor Jian-Xin Xu. She was very fortunate to learn from Professor Xu as a PhD candidate in National University of Singapore in 1998. Since then she has worked with Prof Xu over 20 years. For her, Professor Xu is always the role model with his passion and dedication to science and engineering. His professionalism will be forever remembered. Rest in peace, Professor Xu.

Appendix A. Proof of Proposition 1

The intention of this proof is to show that if $V(t)$ is bounded for all $t \geq 0$, then the constraints are satisfied. In this Appendix, the subscript i for iteration is omitted for all variables as the satisfaction of constraint is investigated for the first iteration where the feed-forward control input is zero:

Define ψ as follows:

$$\psi \triangleq [\mathbf{e}^\top \quad \dot{\mathbf{e}}^\top]^\top. \quad (\text{A.1})$$

Then, σ from (7) can be re-written in terms of ψ as

$$\sigma = \bar{\Omega} \psi, \quad (\text{A.2})$$

where

$$\bar{\Omega} = [\Omega \quad I_n] \psi, \quad (\text{A.3})$$

$$\begin{aligned} \Omega = & \cos^2 \left(\frac{\pi \mathbf{e}^\top \mathbf{e}}{2\varepsilon_b^2} \right) K_1 - \frac{\dot{\varepsilon}_b}{\varepsilon_b} I_n \\ & + \frac{\dot{\varepsilon}_b \varepsilon_b}{\pi \mathbf{e}^\top \mathbf{e}} \sin \left(\frac{\pi \mathbf{e}^\top \mathbf{e}}{\varepsilon_b^2} \right) I_n. \end{aligned} \quad (\text{A.4})$$

For the sake of brevity, a variable $\zeta(\mathbf{e}) \triangleq \Omega \mathbf{e}$ is introduced, where Ω is defined in (A.4). Therefore, σ can be redefined

as

$$\boldsymbol{\sigma} = \dot{\mathbf{e}} + \boldsymbol{\zeta}. \quad (\text{A.5})$$

Finally, a fictitious reference signal is defined as

$$\bar{\mathbf{u}}_r = M(\mathbf{x}_1)M^{-1}(\mathbf{x}_{1,r})\mathbf{u}_r. \quad (\text{A.6})$$

Let us first find the second derivative of \mathbf{e} using (4), it leads to the following dynamics:

$$\begin{aligned} \ddot{\mathbf{e}} &= \dot{\mathbf{x}}_{2,r} - \dot{\mathbf{x}}_2 \\ &= \mathbf{h}(\mathbf{x}_{1,r}, \mathbf{x}_{2,r}) + M^{-1}(\mathbf{x}_{1,r})\mathbf{u}_r - \mathbf{h}(\mathbf{x}_1, \mathbf{x}_2) \\ &\quad - M^{-1}(\mathbf{x}_1)\mathbf{u}. \end{aligned} \quad (\text{A.7})$$

Multiplying $M(\mathbf{x}_1)$ with the time derivative of (A.5) yields

$$\begin{aligned} M(\mathbf{x}_1)\dot{\boldsymbol{\sigma}} &= M(\mathbf{x}_1)(\dot{\mathbf{e}} + \dot{\boldsymbol{\zeta}}) \\ &= M(\mathbf{x}_1)\delta\mathbf{h}(\mathbf{x}_1, \mathbf{x}_2) + M(\mathbf{x}_1)M^{-1}(\mathbf{x}_{1,r})\mathbf{u}_r \\ &\quad - \mathbf{u} + M(\mathbf{x}_1)\dot{\boldsymbol{\zeta}} \\ &= M(\mathbf{x}_1)\delta\mathbf{h}(\mathbf{x}_1, \mathbf{x}_2) + \delta\mathbf{u} + M(\mathbf{x}_1)\dot{\boldsymbol{\zeta}} \\ &= \delta\mathbf{u} - C(\mathbf{x}_1, \mathbf{x}_2)\boldsymbol{\sigma} + \omega, \end{aligned} \quad (\text{A.8})$$

where $\delta\mathbf{u} \triangleq \bar{\mathbf{u}}_r - \mathbf{u}$, $\delta\mathbf{h}(\mathbf{x}_1, \mathbf{x}_2) \triangleq \mathbf{h}(\mathbf{x}_{1,r}, \mathbf{x}_{2,r}) - \mathbf{h}(\mathbf{x}_1, \mathbf{x}_2)$, and $\omega = M(\mathbf{x}_1)\delta\mathbf{h}(\mathbf{x}_1, \mathbf{x}_2) + C(\mathbf{x}_1, \mathbf{x}_2)\boldsymbol{\sigma} + M(\mathbf{x}_1)\dot{\boldsymbol{\zeta}}$.

Fact 1 is established in this section to facilitate the proof.

Fact 1. For $\mathbf{x}_1, \mathbf{x}_2, \mathbf{x}_{1,r}, \mathbf{x}_{2,r}$ and $\boldsymbol{\sigma} \in \mathcal{D}$, there exist positive constants C_s and C_t such that $|\omega| \leq C_t|\boldsymbol{\psi}| + C_s|\boldsymbol{\psi}|^2$, i.e., the value of $|\omega|$ is bounded in the compact set, \mathcal{D} .

Proof. For the proof of Fact 1, consider the following relationships:

$$\begin{aligned} |\omega| &\leq |M(\mathbf{x}_1)(\mathbf{h}(\mathbf{x}_{1,r}, \mathbf{x}_{2,r}) - \mathbf{h}(\mathbf{x}_1, \mathbf{x}_2))| \\ &\quad + |C(\mathbf{x}_1, \mathbf{x}_2)\boldsymbol{\sigma}| + |M(\mathbf{x}_1)\dot{\boldsymbol{\zeta}}(\mathbf{e}, \dot{\mathbf{e}})|. \end{aligned} \quad (\text{A.9})$$

Following Remark 6, it can be shown that there exists $C_s > 0$ such that

$$|\boldsymbol{\sigma}| \leq C_s|\boldsymbol{\psi}|. \quad (\text{A.10})$$

Again $|\mathbf{e}| \leq |\boldsymbol{\psi}|$ and $|\dot{\mathbf{e}}| \leq |\boldsymbol{\psi}|$. Using the Lipschitz continuity of $\mathbf{h}(\cdot, \cdot)$, $\boldsymbol{\zeta}(\cdot, \cdot)$ with the Properties 1, 3, and the boundedness of $\boldsymbol{\sigma}$ from (A.10), it can be shown that there exist positive constants $\frac{1}{2}C_{hz}$ and C_s such that the following inequality holds:

$$\begin{aligned} |\omega| &\leq \frac{1}{2}C_{hz}|\mathbf{e}| + \frac{1}{2}(C_{hz} + C_b)|\dot{\mathbf{e}}| + C_r|\boldsymbol{\psi}| + C_s|\dot{\mathbf{e}}||\boldsymbol{\psi}| \\ &\leq C_t|\boldsymbol{\psi}| + C_s|\boldsymbol{\psi}|^2, \end{aligned} \quad (\text{A.11})$$

where $C_t = C_{hz} + C_b$. Moreover, when $\boldsymbol{\psi} \rightarrow 0$, then $\omega \rightarrow 0$. This completes the Fact 1. \square

Fact 2. When the initial condition of BF-LF V is in a compact set, there exist an invariant set such that $\forall t > 0$, V stays in this invariant set.

Proof. Taking the time derivative of V yields,

$$\begin{aligned} \dot{V} &= \sec^2\left(\frac{\pi\mathbf{e}^\top\mathbf{e}}{2\varepsilon_b^2}\right)\mathbf{e}^\top\dot{\mathbf{e}} - \frac{\dot{\varepsilon}_b}{\varepsilon_b}\sec^2\left(\frac{\pi\mathbf{e}^\top\mathbf{e}}{2\varepsilon_b^2}\right)\mathbf{e}^\top\mathbf{e} \\ &\quad + \frac{2\varepsilon_b\dot{\varepsilon}_b}{\pi}\tan\left(\frac{\pi\mathbf{e}^\top\mathbf{e}}{2\varepsilon_b^2}\right) + \frac{1}{2}\boldsymbol{\sigma}^\top\dot{M}(\mathbf{x}_1)\boldsymbol{\sigma} \\ &\quad + \boldsymbol{\sigma}^\top M(\mathbf{x}_1)\dot{\boldsymbol{\sigma}}. \end{aligned} \quad (\text{A.12})$$

Substituting $\dot{\mathbf{e}}$ from (7) into (A.12) results in canceling $\frac{\dot{\varepsilon}_b}{\varepsilon_b}\sec^2\left(\frac{\pi\mathbf{e}^\top\mathbf{e}}{2\varepsilon_b^2}\right)\mathbf{e}^\top\mathbf{e}$ and $\frac{2\varepsilon_b\dot{\varepsilon}_b}{\pi}\tan\left(\frac{\pi\mathbf{e}^\top\mathbf{e}}{2\varepsilon_b^2}\right)$, followed by substituting (A.8) yields:

$$\begin{aligned} \dot{V} &= \sec^2\left(\frac{\pi\mathbf{e}^\top\mathbf{e}}{2\varepsilon_b^2}\right)\mathbf{e}^\top\boldsymbol{\sigma} - \mathbf{e}^\top K_1\mathbf{e} - \boldsymbol{\sigma}^\top\mathbf{u}^{fb} + \boldsymbol{\sigma}^\top\delta\tilde{\mathbf{u}}^{ff} \\ &\quad + \boldsymbol{\sigma}^\top\omega + \frac{1}{2}\boldsymbol{\sigma}^\top\left(\dot{M}(\mathbf{x}_1) - 2C(\mathbf{x}_1, \mathbf{x}_2)\right)\boldsymbol{\sigma}, \end{aligned} \quad (\text{A.13})$$

where $\delta\tilde{\mathbf{u}}^{ff} = \bar{\mathbf{u}}_r - \tilde{\mathbf{u}}^{ff}$. Again substituting \mathbf{u}^{fb} from (9) into (A.13), results in canceling $\sec^2\left(\frac{\pi\mathbf{e}^\top\mathbf{e}}{2\varepsilon_b^2}\right)\mathbf{e}^\top\boldsymbol{\sigma}$. Because of Property 2, the last term in (A.13) is zero. Therefore, (A.13) can be written as

$$\dot{V} = -\mathbf{e}^\top K_1\mathbf{e} - \boldsymbol{\sigma}^\top K_2\boldsymbol{\sigma} + \boldsymbol{\sigma}^\top\delta\tilde{\mathbf{u}}^{ff} + \boldsymbol{\sigma}^\top\omega. \quad (\text{A.14})$$

Let $\eta_1 = \lambda_{\min}(K_1)$, $\eta_2 = \lambda_{\min}(\bar{\boldsymbol{\Omega}}^\top K_2 \bar{\boldsymbol{\Omega}})$. Substituting (A.2) and (A.10) into (A.14) yields:

$$\begin{aligned} \dot{V} &\leq -\eta_1|\mathbf{e}|^2 - \eta_2|\boldsymbol{\psi}|^2 + C_s|\boldsymbol{\psi}||\delta\tilde{\mathbf{u}}^{ff}| \\ &\quad + C_s C_t |\boldsymbol{\psi}|^2 + C_s^2 |\boldsymbol{\psi}|^3. \end{aligned} \quad (\text{A.15})$$

By considering the positiveness of $|\mathbf{e}|^2$, (A.15) can be written as

$$\dot{V} \leq -\bar{\eta}_2|\boldsymbol{\psi}|^2 + C_s|\boldsymbol{\psi}||\delta\tilde{\mathbf{u}}^{ff}| + C_s^2|\boldsymbol{\psi}|^3, \quad (\text{A.16})$$

where $\bar{\eta}_2 = \eta_2 - C_s C_t$.

When there is no feed-forward control input, i.e., $\mathbf{u}^{ff} = 0$, (A.16) leads to

$$\dot{V} \leq -\bar{\eta}_2|\boldsymbol{\psi}|^2 + \hat{C}_s|\boldsymbol{\psi}| + C_s^2|\boldsymbol{\psi}|^3, \quad (\text{A.17})$$

where $\hat{C}_s = C_s \max_{t \in [0, T_f]} |\bar{\mathbf{u}}_r(t)|$.

For any positive constants $\underline{\nu}$ and $\bar{\nu}$, there exists $\bar{\eta}_2$, \hat{C}_s and C_s^2 , such that $\underline{\nu} \leq |\boldsymbol{\psi}| \leq \bar{\nu}$.

This completes the Fact 2.

Notice that $V(0) = V(\mathbf{e}(0), \boldsymbol{\sigma}(0)) = 0$. $V(t)$ is positive definite and uniformly bounded for any $V(0)$ within the same compact set \mathcal{D} . Hence, it can be concluded that the output constraints are satisfied when there is no feed-forward control input.

This completes the proof. \square

Appendix B. Proof of Theorem 1

Consider the following barrier composite energy function (BCEF)

$$E_i(t) = e^{-\lambda t} V_{i-1}(t) + \int_0^t e^{-\lambda \tau} \delta \mathbf{u}_i^{ff} \Gamma(\tau) \delta \mathbf{u}_i^{ff}(\tau) d\tau$$

$$\forall t \in [0, T_f], \quad i \in \mathcal{N}, \lambda > 0, \text{ and } V_0(t) = 0. \quad (\text{B.1})$$

Note that $\delta \mathbf{u}_i^{ff} = \bar{\mathbf{u}}_r - \mathbf{u}_i^{ff}$, where $\bar{\mathbf{u}}_r$ is defined in (A.6).

The BCEF (B.1) is composed of a time weighted function of BF-LF (10) and the \mathcal{L}_e^2 norm of the error in the feed-forward control input. A novel induction-based proof technique is employed to show that the constraints are not violated in any iterations.

It can be shown that for a given $\Delta_0 > 0$ and $\lambda > 0$, if $E(t) \leq \Delta_0$ then $\psi(t)$ belongs to a compact set \mathcal{D} such that there exists $\Delta_1 > 0$ satisfying $\|\psi\|_s^2 \leq \Delta_1$. The following proof technique is based on induction, which has two main steps.

The first step is to show that the constraints are satisfied at the first iteration. Hence, E_1 is bounded and uniformly continuous. Using Proposition 1, the output trajectories at first iteration satisfy the constraints. Therefore, assume $\psi_1(t)$ belongs to the compact set \mathcal{D} .

The next step in the proof is to show that $E_{j+1}(t) \leq E_j(t)$ and is bounded for any bounded E_j . A bounded E_j with a bounded V_{j-1} indicates that \mathbf{u}_j^{ff} belongs to \mathcal{L}_e^2 .

Assume that at the j th iteration, $\max_{t \in [0, T_f]} E_j(t) \leq \Delta_0$ and $\|\psi_{j-1}\|_s^2 \leq \Delta_1$. We will show that at the $(j+1)$ th iteration, $\max_{t \in [0, T_f]} E_{j+1}(t) \leq \Delta_0$ and $\|\psi_j\|_s^2 \leq \Delta_1$. The construction of the compact set \mathcal{D} will ensure that for all $t \in [0, T_f]$, the constraints are satisfied for all iterations.

For the sake of brevity, the variable t is omitted whenever appropriate.

At the $(j+1)$ th iteration, the difference of the BCEF between two consecutive iterations is given by $\Delta E_{j+1} = E_{j+1} - E_j$. Consequently, it has

$$\Delta E_{j+1} = e^{-\lambda t} (V_j - V_{j-1})$$

$$+ \int_0^t e^{-\lambda \tau} \left(|\delta \mathbf{u}_{j+1}^{ff}|^2 - |\delta \mathbf{u}_j^{ff}|^2 \right) d\tau. \quad (\text{B.2})$$

The first term in (B.2) can be expanded to an integral form, followed by substituting for V_j from (10) resulting in

$$e^{-\lambda t} V_j = -\lambda \int_0^t e^{-\lambda \tau} V_j d\tau + \int_0^t e^{-\lambda \tau} \dot{V}_j d\tau$$

$$\leq -\frac{\lambda}{\pi} \int_0^t e^{-\lambda \tau} \varepsilon_b^2 \tan\left(\frac{\pi \mathbf{e}_j^\top \mathbf{e}_j}{2\varepsilon_b^2}\right) d\tau$$

$$- \lambda \int_0^t e^{-\lambda \tau} \boldsymbol{\sigma}_j^\top M(\mathbf{x}_j) \boldsymbol{\sigma}_j d\tau$$

$$+ \int_0^t e^{-\lambda \tau} \dot{V}_j d\tau. \quad (\text{B.3})$$

For the proof by induction, it is assumed that the constraints are satisfied for j th iteration. Convergence of ψ is equivalent to the convergence in \mathbf{e} and $\dot{\mathbf{e}}$. Therefore, by considering the positiveness of $\tan\left(\frac{\pi \mathbf{e}_j^\top \mathbf{e}_j}{2\varepsilon_b^2}\right)$ and substituting for (A.2) in (B.3) yields

$$e^{-\lambda t} V_j \leq -\lambda \int_0^t e^{-\lambda \tau} \mu |\psi_j|^2 d\tau + \int_0^t e^{-\lambda \tau} \dot{V}_j d\tau, \quad (\text{B.4})$$

where $\mu(t) = \lambda_{\min}(\bar{\Omega}^\top M(\mathbf{x}_j) \bar{\Omega}) \geq \kappa_0(t)$. It can be shown that for any given $\varepsilon_b(t)$ and $\mathbf{y}_r(t)$, there exists a K_1 such that there exists a positive constant δ where $\kappa(t) \geq \delta > 0$.

Substituting \dot{V}_j from (A.16) into (B.4) yields

$$e^{-\lambda t} V_j \leq -\lambda \int_0^t e^{-\lambda \tau} \mu |\psi_j|^2 d\tau - \bar{\eta}_2 \int_0^t e^{-\lambda \tau} |\psi_j|^2 d\tau$$

$$+ C_s^2 \int_0^t e^{-\lambda \tau} |\psi_j|^3 d\tau$$

$$+ C_s \int_0^t e^{-\lambda \tau} |\psi_j| |\delta \tilde{\mathbf{u}}_j^{ff}| d\tau. \quad (\text{B.5})$$

By using completion of squares, we can show that there exists a $\beta > 0$ such that

$$|\psi_j| |\delta \tilde{\mathbf{u}}_j^{ff}|$$

$$= \sqrt{\beta} |\psi_j| \frac{1}{\sqrt{\beta}} |\delta \tilde{\mathbf{u}}_j^{ff}| \leq \frac{\beta}{2} |\psi_j|^2 + \frac{1}{2\beta} |\delta \tilde{\mathbf{u}}_j^{ff}|^2. \quad (\text{B.6})$$

Substituting (B.6) back into (B.5) yields

$$e^{-\lambda t} V_j \leq -\lambda \int_0^t e^{-\lambda \tau} \mu |\psi_j|^2 d\tau + \int_0^t e^{-\lambda \tau} N(|\psi_j|) d\tau$$

$$+ \frac{C_s}{2\beta} \int_0^t e^{-\lambda \tau} |\delta \tilde{\mathbf{u}}_j^{ff}|^2 d\tau, \quad (\text{B.7})$$

where $N(|\psi_j|) = \left(-\bar{\eta}_2 + \frac{C_s \beta}{2}\right) |\psi_j|^2 + C_s^2 |\psi_j|^3$ is a polynomial function in ψ .

Secondly, the ILC update law (6) can be expressed as

$$\bar{\mathbf{u}}_r - \mathbf{u}_{j+1}^{ff} = \bar{\mathbf{u}}_r - \tilde{\mathbf{u}}_j^{ff} - q\Gamma \dot{\mathbf{e}}_j. \quad (\text{B.8})$$

From (A.7), using the relation $M^{-1}(\mathbf{x}_{1,r}) \mathbf{u}_r = M^{-1}(\mathbf{x}_{1,j}) \bar{\mathbf{u}}_r$, $\dot{\mathbf{e}}_j$ can be expressed as

$$\dot{\mathbf{e}} = \delta \mathbf{h}(\mathbf{x}_{1,j}, \mathbf{x}_{2,j}) + M^{-1}(\mathbf{x}_{1,r}) \mathbf{u}_r - M^{-1}(\mathbf{x}_{1,j}) \mathbf{u}$$

$$= \delta \mathbf{h}(\mathbf{x}_{1,j}, \mathbf{x}_{2,j}) + M^{-1}(\mathbf{x}_{1,j}) \delta \mathbf{u}. \quad (\text{B.9})$$

Substituting (B.9) into (B.8) yields

$$\delta \mathbf{u}_{j+1}^{ff} = P(\mathbf{x}_{1,j}) \delta \tilde{\mathbf{u}}_j^{ff} + \mathbf{w}_j, \quad (\text{B.10})$$

where $P(\mathbf{x}_{1,j}) = I_n - q\Gamma M^{-1}(\mathbf{x}_{1,j})$ and

$$\mathbf{w}_j = -q\Gamma \delta \mathbf{h}(\mathbf{x}_{1,j}, \mathbf{x}_{2,j}) + q\Gamma M^{-1}(\mathbf{x}_{1,j}) \left(\delta \tilde{\mathbf{u}}_j^{ff} - \delta \mathbf{u}_j \right). \quad (\text{B.11})$$

It is possible to find $\Gamma > 0$ and $q > 0$ such that $|P(\mathbf{x}_{1,j})| < \rho < 1$. This leads to the satisfaction of convergence condition (11) in Theorem 1.

Using the assumption that the constraints are satisfied on j th iteration, there exists $U_b > 0$ such that $|\mathbf{u}_j^{fb}| \leq U_b |\psi_j|$. It can be further assumed that $q\Gamma\mathbf{h}(\cdot, \cdot)$ are Lipschitz continuous with Lipschitz constants $\frac{1}{2}C_h > 0$ and using Property 1, there exists a μ_3 such that

$$|q\Gamma\delta\mathbf{h}(\mathbf{x}_{1,j}, \mathbf{x}_{2,j})| \leq \frac{1}{2}C_h(|\dot{\mathbf{e}}_j| + |\mathbf{e}_j|) \leq C_h|\psi_j| \quad (\text{B.12})$$

$$|q\Gamma M^{-1}(\mathbf{x}_{1,j})| \leq \mu_3. \quad (\text{B.13})$$

Substituting (B.12) and (B.13) in (B.11) yields

$$|\mathbf{w}_j| \leq C_{hb}|\psi_j|, \quad (\text{B.14})$$

where $C_{hb} = C_h + \mu_3 U_b$. Using Lemma 1 and substituting (B.10) on the expression $(\delta\mathbf{u}_{j+1}^{ff\top} \delta\mathbf{u}_{j+1}^{ff} - \delta\mathbf{u}_j^{ff\top} \delta\mathbf{u}_j^{ff})$, followed by (B.6) and (B.14) gives:

$$\begin{aligned} & \delta\mathbf{u}_{j+1}^{ff\top} \delta\mathbf{u}_{j+1}^{ff} - \delta\mathbf{u}_j^{ff\top} \delta\mathbf{u}_j^{ff} \\ & \leq \delta\mathbf{u}_{j+1}^{ff\top} \delta\mathbf{u}_{j+1}^{ff} - \delta\tilde{\mathbf{u}}_j^{ff\top} \delta\tilde{\mathbf{u}}_j^{ff} \\ & \leq -(I_n - |P(\mathbf{x}_{1,j})|^2) |\delta\tilde{\mathbf{u}}_j^{ff}|^2 + |\mathbf{w}_j|^2 + 2\rho|\mathbf{w}_j| |\delta\tilde{\mathbf{u}}_j^{ff}| \\ & \leq -(\lambda_p - C_u) |\delta\tilde{\mathbf{u}}_j^{ff}|^2 + Q(|\psi_j|), \end{aligned} \quad (\text{B.15})$$

where $\lambda_p = |I_n - |P(\mathbf{x}_{1,j})|^2|$, $C_u = \frac{\rho C_{hb}}{\beta}$, $Q(|\psi_j|) = (C_{hb}^2 + \rho C_{hb}\beta) |\psi_j|^2$. Moreover, $|P(\mathbf{x}_j)| < \rho < 1$, leads to $\lambda_p > 0$.

Finally, substituting (B.7) and (B.15) back into (B.2) and considering the positiveness of V_{j-1} yields

$$\begin{aligned} \Delta E_{j+1} & \leq -\lambda \int_0^t e^{-\lambda\tau} \mu |\psi_j|^2 d\tau + \int_0^t e^{-\lambda\tau} R(|\psi_j|) d\tau \\ & \quad - (\lambda_p - C_{lu}) \int_0^t e^{-\lambda\tau} |\delta\tilde{\mathbf{u}}_j^{ff}|^2 d\tau, \end{aligned} \quad (\text{B.16})$$

where $R(|\psi_j|) = N(|\psi_j|) + Q(|\psi_j|)$, $C_{lu} = C_u + \frac{C_s}{2\beta}$ and $R(|\psi_j|) = r_0 |\psi_j|^2 + C_s^2 |\psi_j|^3$ with $r_0 = -\eta_2 + \beta(\frac{C_s}{2} + \rho C_{hb}) + C_{hb}^2$.

For any given $|\psi_j| \in \mathcal{D}$, it is possible to show there exists a $\lambda > \frac{1}{\mu}(r_0 + C_s^2 \Delta_1)$ and $\lambda_p > C_{lu}$, such that $\Delta E_{j+1} \leq 0$. Therefore, there exists $N_\lambda > 0$ and $N_\beta > 0$ such that

$$\Delta E_{j+1} \leq - \int_0^t e^{-\lambda\tau} [N_\lambda |\psi_j|^2 + N_\beta |\delta\tilde{\mathbf{u}}_j^{ff}|^2] d\tau. \quad (\text{B.17})$$

Hence, it is possible to conclude $E_{j+1} \leq \Delta_0$ and belongs to the compact set \mathcal{D} . By using induction, all the trajectories ψ_{j+1} satisfies the constraints for all $j = 1, 2, 3, \dots$

Moreover E_{j+1} is nonincreasing along the iteration axis and satisfies (B.17). Hence,

$$\begin{aligned} & \lim_{j \rightarrow \infty} \int_0^{T_j} e^{-\lambda\tau} [N_\lambda |\psi_j|^2 + N_\beta |\delta\tilde{\mathbf{u}}_j^{ff}|^2] d\tau = 0, \\ & \lim_{j \rightarrow \infty} \|\psi_j\|_{\mathcal{L}_e^2} = 0 \text{ and } \lim_{j \rightarrow \infty} \|\delta\tilde{\mathbf{u}}_j^{ff}\|_{\mathcal{L}_e^2} = 0. \end{aligned} \quad (\text{B.18})$$

Thus, point-wise convergence is achieved. In addition, the convergence in the sense of \mathcal{L}_e^2 norm can be shown as an equivalent to \mathcal{L}^2 norm.

The uniformly continuity and boundedness of ψ_i can be ensured. Hence, uniform convergence of ψ_i is ensured when $i \rightarrow \infty$. Hence, the total control input, \mathbf{u}_i is uniformly bounded for all iterations. Similarly, when $i \rightarrow \infty$, $\bar{\mathbf{u}}_r \rightarrow \mathbf{u}_r$ as $\mathbf{x}_{1,i} \rightarrow \mathbf{x}_{1,r}$. Therefore, $\tilde{\mathbf{u}}_j^{ff} \rightarrow \mathbf{u}_r$ in \mathcal{L}^2 norm. Hence, it can be concluded that $\lim_{i \rightarrow \infty} \mathbf{u} \rightarrow \mathbf{u}_r$ as the feedback disappears when tracking error goes to zero. This completes the proof.

References

- [1] S. Arimoto, S. Kawamura and F. Miyazaki, Bettering operation of robots by learning, *J. Robot. Syst.* **1**(2) (1984) 123-140.
- [2] D. A. Bristow, M. Tharayil and A. G. Alleyne, A survey of iterative learning control, *IEEE Control Systems* **26**(3) (2006) 96-114.
- [3] H.-S. Ahn, Y. Chen and K. L. Moore, Iterative learning control: Brief survey and categorization, *IEEE Trans. Syst. Man Cybern. C Appl. Rev.* **37**(6) (2007) 1099.
- [4] Y. Wang, F. Gao and F. J. Doyle, Survey on iterative learning control, repetitive control, and run-to-run control, *J. Process Cont.* **19**(10) (2009) 1589-1600.
- [5] S.-H. Zhou, J. Fong, V. Crocher, Y. Tan, D. Oetomo and I. Mareels, Learning control in robot-assisted rehabilitation of motor skills — a review, *Journal of Control and Decision* **3**(1) (2016) 19-43.
- [6] Z. Bien and J.-X. Xu, *Iterative Learning Control: Analysis, Design, Integration and Applications* (Springer Science & Business Media, New York, 2012).
- [7] J.-X. Xu and Y. Tan, *Linear and Nonlinear Iterative Learning Control* (Springer, New York, 2003).
- [8] J.-X. Xu, A survey on iterative learning control for nonlinear systems, *Int. J. Control* **84**(7) (2011) 1275-1294.
- [9] T.-Y. Kuc, J. S. Lee and K. Nam, An iterative learning control theory for a class of nonlinear dynamic system, *Automatica* **28**(6) (1992) 1215-1221.
- [10] M. French and E. Rogers, Non-linear iterative learning by an adaptive lyapunov technique, *Int. J. Control* **73**(10) (2000) 840-850.
- [11] C. Ham, Z. Qu and J. Kaloust, Nonlinear learning control for a class of nonlinear systems, *Automatica* **37**(3) (2001) 419-428.
- [12] J.-X. Xu and Y. Tan, A composite energy function-based learning control approach for nonlinear systems with time-varying parametric uncertainties, *IEEE Trans. Autom. Control* **47**(11) (2002) 1940-1945.
- [13] J.-X. Xu and J. Xu, On iterative learning from different tracking tasks in the presence of time-varying uncertainties, *IEEE Trans. Syst. Cybern. Part B* **34**(1) (2004) 589-597.
- [14] J.-X. Xu, Y. Tan and T.-H. Lee, Iterative learning control design based on composite energy function with input saturation, *Automatica* **40** (2004) 1371-1377.
- [15] J.-X. Xu, X. Jin and D. Huang, Composite energy function-based iterative learning control for systems with nonparametric uncertainties, *Int. J. Adapt. Control Signal Process.* **28**(1) (2014) 1-13.
- [16] Y. Tan, H.-H. Dai, D. Huang and J.-X. Xu, Unified iterative learning control schemes for nonlinear dynamic systems with nonlinear input uncertainties, *Automatica* **48**(12) (2012) 3173-3182.
- [17] I. Díaz, J. J. Gil and E. Sánchez, Lower-limb robotic rehabilitation: Literature review and challenges, *J. Robot.* **2011** (2011) 408-418.

12 G. Sebastian et al.

- [18] L. Marchal-Crespo and D. J. Reinkensmeyer, Review of control strategies for robotic movement training after neurologic injury, *J. Neuroeng. Rehabil.* **6**(1) (2009) 20.
- [19] M. Sun, D. Wang and P. Chen, Repetitive learning control of nonlinear systems over finite intervals, *Sci. China Ser. F* **53**(1) (2010) 115–128.
- [20] D. Bonvin, Control and optimization of batch processes, *IEEE Control Syst.* **26**(6) (2006) 34–45.
- [21] J. Krüger, T. K. Lien and A. Verl, Cooperation of human and machines in assembly lines, *CIRP Annals-Manufacturing Technology* **58**(2) (2009) 628–646.
- [22] J.-X. Xu and X. Jin, State-constrained iterative learning control for a class of MIMO systems, *IEEE Trans. Autom. Control* **58**(5) (2013) 1322–1327.
- [23] X. Jin and J.-X. Xu, Iterative learning control for output-constrained systems with both parametric and nonparametric uncertainties, *Automatica* **49**(8) (2013) 2508–2516.
- [24] X. Jin and J.-X. Xu, A barrier composite energy function approach for robot manipulators under alignment condition with position constraints, *Int. J. Robust Nonlin. Control* **24**(17) (2014) 2840–2851.
- [25] H. K. Khalil, *Nonlinear Systems*, 3 edn. (Prentice Hall, Upper Saddle River, New Jersey, 2002).
- [26] G. Sebastian, Y. Tan, D. Oetomo and I. Mareels, Feedback-based iterative learning design and synthesis with output constraints for robotic manipulators, *IEEE Control Syst. Lett.* **2** (2018) 513–518.
- [27] F. L. Lewis, D. M. Dawson and C. T. Abdallah, *Robot Manipulator Control: Theory and Practice*, 2nd edn. (Marcel Dekker, New York, 2004).
- [28] H.-S. Ahn, C.-H. Choi and K.-B. Kim, Iterative learning control for a class of nonlinear systems, *Automatica* **29**(6) (1993) 1575–1578.
- [29] J.-X. Xu and R. Yan, On initial conditions in iterative learning control, *IEEE Trans. Autom. Control* **50**(9) (2005) 1349–1354.
- [30] Y. Tan, S. Yang and J. Xu, On p-type iterative learning control for nonlinear systems without global lipschitz continuity condition, in *American Control Conf. (ACC), 2015*, IEEE (2015), pp. 3552–3557.
- [31] K. P. Tee, S. S. Ge and E. H. Tay, Barrier Lyapunov functions for the control of output-constrained nonlinear systems, *Automatica* **45**(4) (2009) 918–927.
- [32] K. B. Ngo, R. Mahony and Z.-P. Jiang, Integrator backstepping using barrier functions for systems with multiple state constraints, in *Proc. 44th IEEE Conf. Decision and Control*, IEEE (2005), pp. 8306–8312.
- [33] J. Fong, V. Crocher, Y. Tan, D. Oetomo and I. Mareels, EMU: A transparent 3d robotic manipulandum for upper-limb rehabilitation, in *Rehabilitation Robotics (ICORR), 2017 Int. Conf.*, IEEE (2017), pp. 771–776.
- [34] J. Wu, J. Wang and Z. You, An overview of dynamic parameter identification of robots, *Robot. Comput. Integr. Manuf.* **26**(5) (2010) 414–419.



Gijo Sebastian is a PhD student at The University of Melbourne. He received B Tech from University of Kerala, India in 2010 and M Tech from Indian Institute of Technology Madras, India in 2013. He worked with Applied Materials, India (2010–2011) and GKN Aerospace, India (2013–2015). He is a student member of Institute of Electrical and Electronics Engineers. His research interests include control theory and application, robotics and human motor learning.



Ying Tan is an Associate Professor and Reader in the Department of Electrical and Electronic Engineering at The University of Melbourne, Australia. She received her Bachelors degree from Tianjin University, China, in 1995, and her PhD from the National University of Singapore in 2002. She joined McMaster University in 2002 as a postdoctoral fellow in the Department of Chemical Engineering.

Since 2004, she has been with the University of Melbourne. She was awarded an Australian Postdoctoral Fellow (2006–2008) and a Future Fellow (2009–2013) by the Australian Research Council. Her research interests are in intelligent systems, nonlinear control systems, real time optimization, sampled-data distributed parameter systems and formation control.



Denny Oetomo is an Associate Professor at the Department of Mechanical Engineering, University of Melbourne. He graduated BEng (Honours 1, 1998) from Australian National University and PhD (Mechanical Engineering, 2004) from National University of Singapore. He was a Research Fellow with the Department of Mechanical Engineering, Monash University (2004–2006), a postdoctoral fellow in a European Union Project at INRIA Sophia-Antipolis, France (Nov 2006–Jan 2008).

His research interests are in the area of robotic manipulation, physical human–robot interaction and assistive robotics, with a focus on the clinical applications of robotics.



Iven Mareels is the Lab Director at IBM Research Australia since Feb 2018. He is also an honorary Professor at the University of Melbourne. Prior to this, he was the Dean of Engineering at the University of Melbourne (2007–2018).

Iven is a Commander in the Order of the Crown of Belgium, a Fellow of The Academy of Technological Sciences and Engineering Australia; The Institute of Electrical and Electronics Engineers (USA), the International Federation of Automatic Control and Engineers Australia. He is a Foreign Member of the Royal Flemish Academy of Belgium for Science and the Arts. He has co-authored five books, and in excess of 130 journal papers/book chapters, and about 250 conference papers.